Supporting Information

$Cu/ZnAl_xO_y$ synthesized by sol-gel method with polyacrylic acid as catalysts for glycerol hydrogenolysis

Table of Contents

Table S1. Compositions (Cu, Al, Zn contents), Cu_{exp} and Cu mean particle size estimated by N_2O chemisorption, ZnO and Cu mean crystallite size estimated by XRD for the catalysts.

Entry	Catalysts	Stoichiometry	Cu[a] (wt%)	Al[a] (wt%)	Zn[a] (wt%)	Cu_{exp} ($m^2_{Cu}\ g^{-1}_{Cu}$)[c]	d_{Cu} (nm)[c], N_2O	d_{Cu} (nm)[d], XRD	d_{ZnO} (nm)[d], XRD
1	4Cu-11Al-S1	$Cu_{0.1}Zn_{1.0}Al_{0.5}$	4.3	10.6	55.3	131.2	5	4	5
2	9Cu-11Al-S1	$Cu_{0.2}Zn_{1.0}Al_{0.5}$	9.1	10.6	52.2	88.5	7	7	5
3	11Cu-11Al-S1	$Cu_{0.2}Zn_{1.0}Al_{0.6}$	10.6	10.7	46.9	83.8	8	9	4
4	18Cu-24Al-S1	$Cu_{1.2}Zn_{1.0}Al_{3.7}$	17.8	23.5	15.5	76.1	9	13	2
5	25Cu-16Al-S1	$Cu_{0.9}Zn_{1.0}Al_{1.4}$	25.0	16.5	28.8	63.0	11	12	3
6	21Cu-S1	$Cu_{0.3}Zn$	20.6	0	63.4	14.6	46	16	20
7	11Cu-11Al-S1-P	$Cu_{0.2}Zn_{1.0}Al_{0.6}$	11.3	11.0	47.7	-	-	36	13
8a	11Al	$Zn_{1.0}Al_{0.5}$	-	11.7[e]	55.7[e]	-	-	-	8
8b	26Cu/11Al-S2	$Cu_{0.7}$ / $Zn_{1.0}Al_{0.7}$	26.1	11.4 (11)[f]	37.1 (48)[f]	51.2	13	9	4
9a	22Al	$Zn_{1.0}Al_{2.5}$	-	25.9[e]	25.5[e]	-	-	-	-
9b	16Cu/22Al-S2	$Cu_{0.8}$ / $Zn_{1.0}Al_{2.4}$	16.5	22.2 (21)[f]	22.4 (20)[f]	52.5	13	5	-

[a] Based on ICP analysis; [b] based on elemental analysis; [c] based on N_2O chemisorption; [d] based on XRD diffractogram, [e] after calcination at 400 °C; [f] theoretical value

Table S2. Catalysts stoichiometries estimated by ICP and EDX analyses.

Catalysts	ICP[a]	SEM[b]
11Cu-11Al-S1	$Cu_{0.2}Zn_{1.0}Al_{0.6}$	$Cu_{0.2}Zn_{1.0}Al_{0.4}$
18Cu-24Al-S1	$Cu_{1.2}Zn_{1.0}Al_{3.7}$	$Cu_{1.2}Zn_{1.0}Al_{3.3}$
26Cu/11Al-S2	$Cu_{0.7}$ / $Zn_{1.0}Al_{0.7}$	$Cu_{0.6}$ / $Zn_{1.0}Al_{1.0}$

[a] based on ICP analyses; estimated error $n_{Cu}/n_{Zn} \pm 0.1$; $n_{Al}/n_{Zn} \pm 0.1$
[b] based on EDX analyses; homogeneity $n_{Cu}/n_{Zn} \pm 0.1$; $n_{Al}/n_{Zn} \pm 0.2$

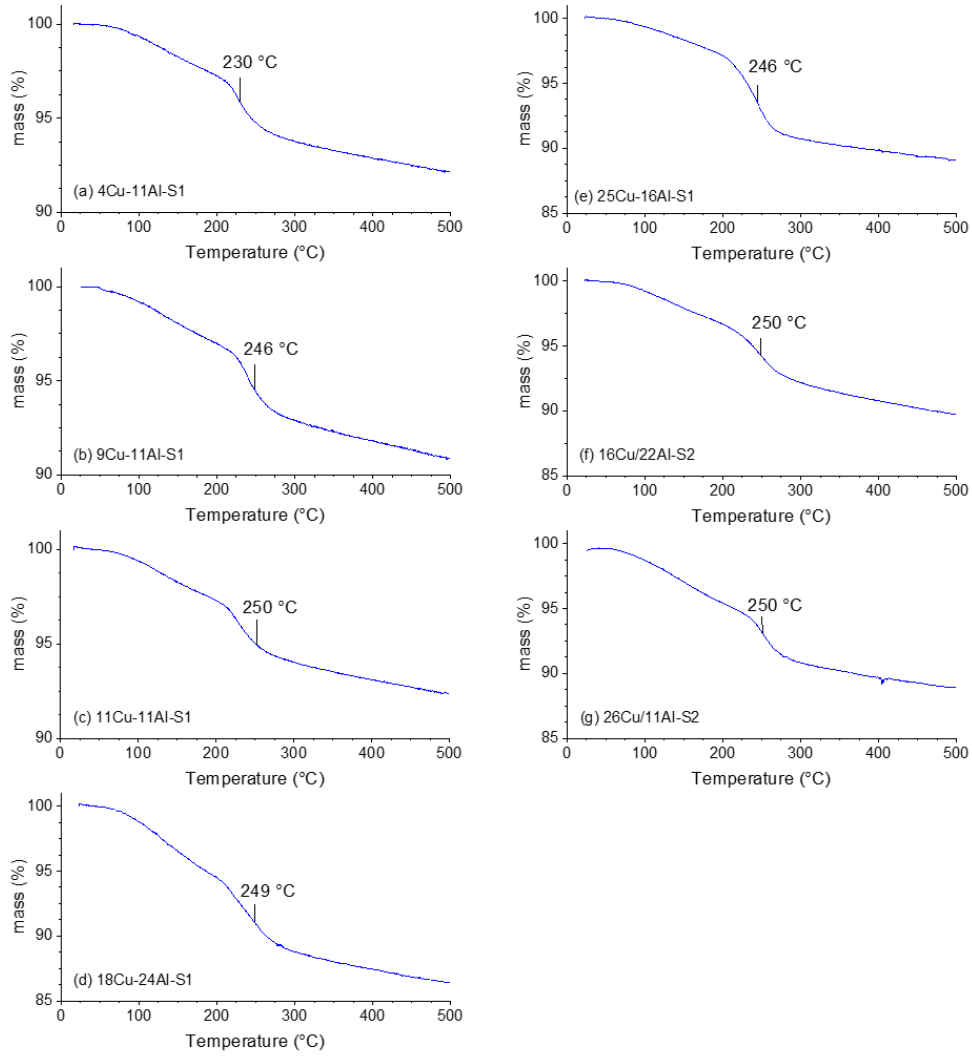

Figure S1. Evolution of mass (%) in function of temperature (°C) during TGA (5 °C min^{-1}) under 3% v/v H_2/Ar for (a) 4Cu-11Al-S1, (b) 9Cu-11Al-S1, (c) 11Cu-11Al-S1, (d) 18Cu-24Al-S1, (e) 25Cu-16Al-S1, (f) 16Cu/22Al-S2 and (g) 26Cu/11Al-S2.

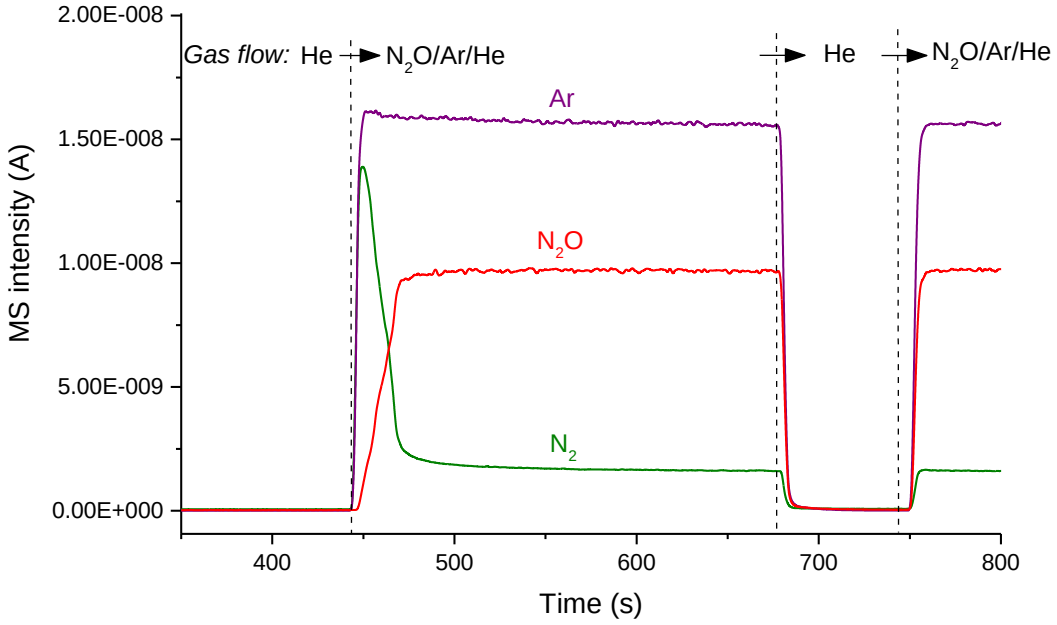

Figure S2. N_2O experiment for 9Cu-11Al-S1 as representative example. Temporal evolution of MS intensity profiles associated with m/z = 40 (Ar), 44 (N_2O) and 28 (N_2).

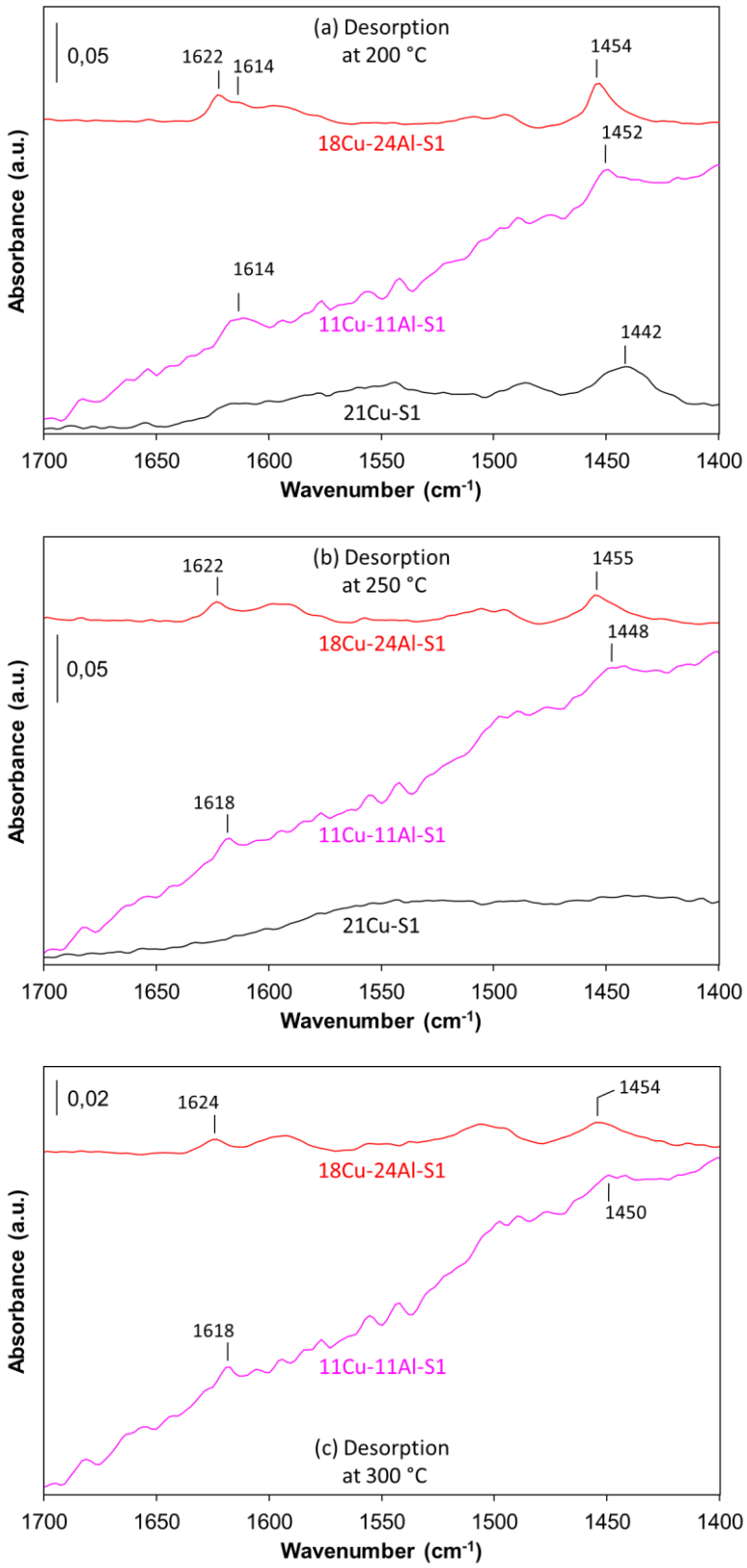

Figure S3. FTIR spectra of adsorbed pyridine following outgas treatment at (a) 200 °C, (b) 250 °C and (c) 300 °C for 18Cu-24Al-S1, 11Cu-11Al-S1 and 21Cu-S1 (Spectra normalized to 10 mg cm^{-2}).

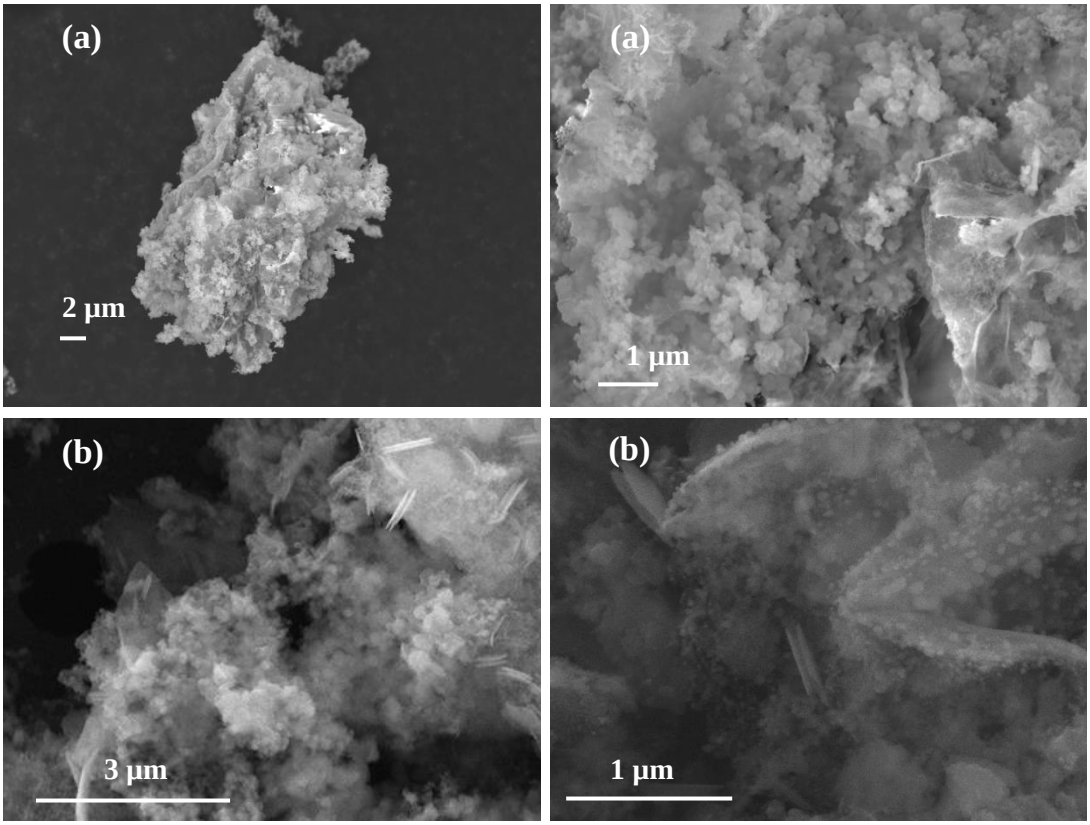

Figure S4. Representative SEM images associated with (a) 26Cu/11Al-S2 and (b) 16Cu/22Al-S2.

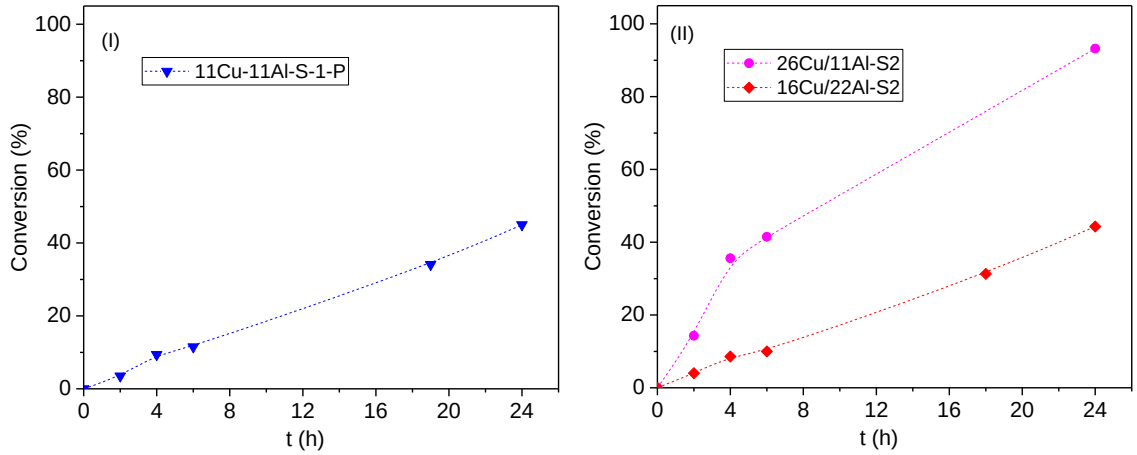

Figure S5. Temporal evolution of the conversion of glycerol (%) for the catalysts synthesized by (I) 11Cu-11Al-S1-P and (II) S2 method. Aqueous solution of glycerol (100 mL of 0.23 M glycerol in water; 500 mg of catalyst, 200°C and 30 bar of H_2).

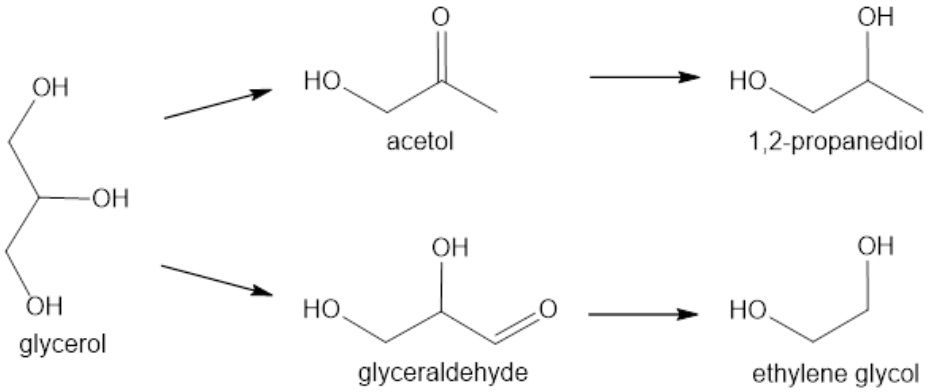

Scheme S1. Reaction pathway observed for the hydrogenolysis of glycerol over $Cu/ZnAl_xO_y$.

Table S3. Results for the hydrogenolysis of glycerol.

Entry	Catalysts	Y_{PDO} (%)[a]	Cu efficiency n_{gly}/n_{Cu} (mol_{gly} mol_{Cu}^{-1})[a,b,c]	Initial rate V_0 ($mmol_{gly}$ g_{Cu}^{-1} h^{-1})[b,d]	Productivity $n_{gly}/m_{catalyst}$ ($mmol_{gly}$ g^{-1})[a,e]
1	4Cu-11Al-S1	20	14.3	28.0	9.8
2	9Cu-11Al-S1	45	16.9	11.1	24.1
3	11Cu-11Al-S1	61	20.6	20.4	34.4
4	18Cu-24Al-S1	67	13.2	13.1	36.9
5	25Cu-16Al-S1	80	11.3	15.1	44.5
6	21Cu-S1	36	5.7	3.7	18.6
7	11Cu-11Al-S1-P	41	11.8	7.7	20.9
8	26Cu/11Al-S2	72	10.6	13.4	43.3
9	16Cu/22Al-S2	40	7.9	5.1	29.7

[a] After 24 h reaction: Aqueous solution of glycerol (100 mL of 0.23 M glycerol in water; 500 mg of catalyst, 200°C and 30 bar of H_2).
[b] Values based on the total amount of Cu in the sample (based on the ICP analysis and the mass of catalyst employed during the reaction)
[c] The Values are given with an absolute accuracy of ± 0.4 mol_{gly} mol_{Cu}^{-1}
[d] The Values are given with an absolute accuracy of ± 0.3 $mmol_{gly}$ g_{Cu}^{-1} h^{-1}
[e] The Values are given with an absolute accuracy of ± 1 $mmol_{gly}$ g^{-1}

The TOF (h^{-1}) values are directly linked to Cu efficiency, with TOF (h^{-1}) = Cu efficiency / 24

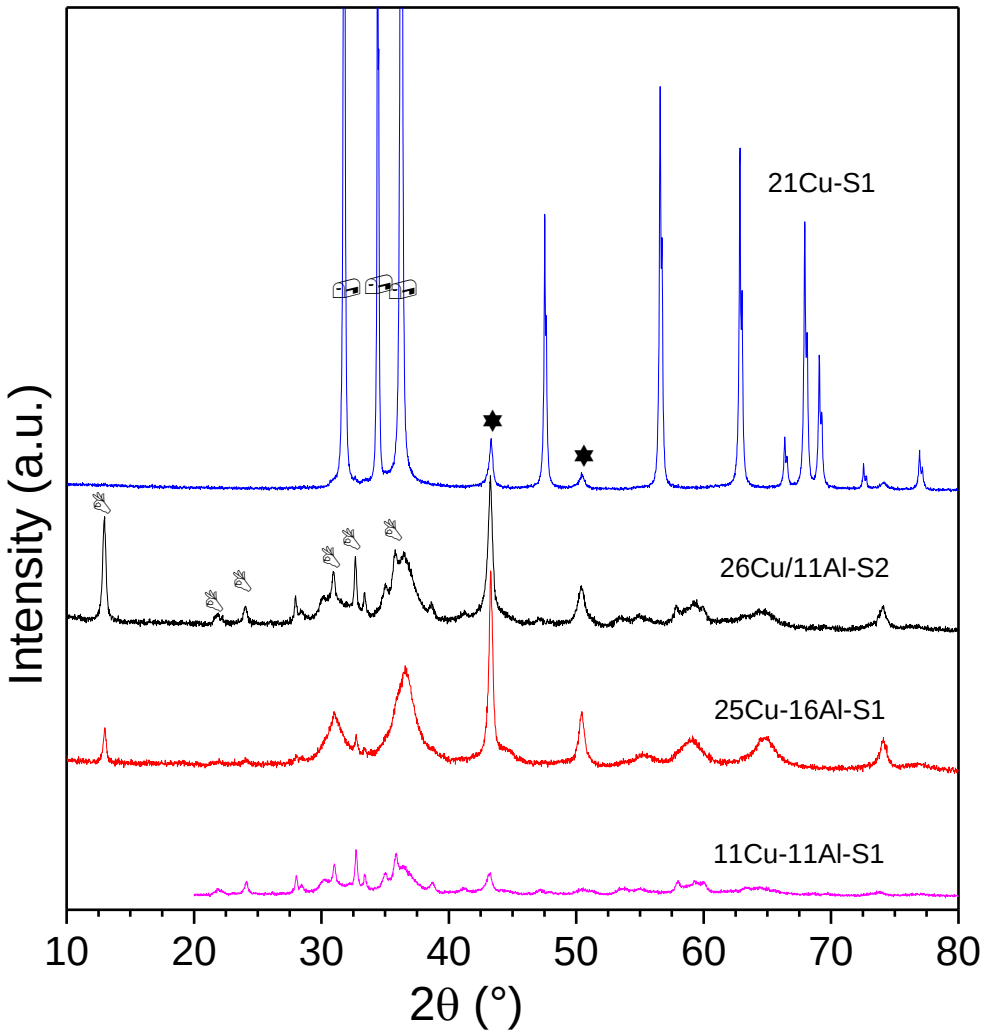

Figure S6. XRD diffractograms associated with11Cu-11Al-S1, 25Cu-16Al-S1, 26Cu/11Al-S2 and 21Cu-S1 after reactions. Symbols refer to the main peaks associated with (●) ZnO (P63mc, PDF 01-079-0205), (✸) Cu (Fm-3m, PDF 04-13-9963) and (▼) $Zn_5(CO_3)_2(OH)_6$ (C21m, PDF 00-019-1458).

Table S4. Surface area and mean Cu crystallite size of representative catalysts, before and after reaction.

Catalysts	Before reaction		After reaction		Leaching (% wt.)[c]		
	Surface area (m^2 g^{-1})[a]	d_{Cu} (nm)[b]	Surface area (m^2 g^{-1})[a]	d_{Cu} (nm)[b]	Cu	Al	Zn
11Cu-11Al-S1	76	9	146	21	<0.1	<0.1	10
25Cu-16Al-S1	97	12	142	18	<0.1	<0.1	10 (1)[d]
21Cu-S1	24	16	33	28	<0.1	<0.1	10
26Cu/11Al-S2	111	9	115	20	<0.1	<0.1	15

[a]based on N_2 physisorption, [b]based on XRD analysis, [c] % of the initial amount of metal lost during the reaction, based on ICP analyses of the solution after reaction, [d] value after Test 2.